

Modelization of Photoacoustic Trace Gases Sensors

B. Parvitte*, C. Risser, R. Vallon and V. Zeninari

Groupe de Spectrométrie Moléculaire et Atmosphérique, UMR CNRS 7331, UFR Sciences Exactes et Naturelles, Université de Reims Champagne-Ardenne, Moulin de la Housse, BP 1039, 51687 Reims Cedex 2

*Corresponding author: bertrand.parvitte@univ-reims.fr

Abstract: This paper aims to demonstrate the simulation of photoacoustic signals using FEM software. The “acoustics” module of the software Comsol Multiphysics is used to calculate the response of a differential Helmholtz resonator cell. In a second part a preliminary result obtained with the “thermoacoustics” module is also presented.

Keywords: Photoacoustic signals, Helmholtz cells, Acoustics module.

1. Introduction

Photoacoustic (PA) spectroscopy is a very sensitive method for gas monitoring [1]. It consists of sending modulated radiation into a sample gas cell containing a microphone. Any absorbed radiation will be, in general, converted to thermal energy of the gas due to collisions thus leading to a modulated pressure detectable with a microphone. As any spectroscopic system, a PA detector presents the main advantage of being highly selective. Moreover PA sensors are robust devices that can easily be implemented for in situ monitoring. Thanks to resonant cells and differential measurement techniques, PA sensors have shown excellent sensitivities on the level of party-per-billion (ppb) for most atmospheric gases [2–3]. These results are comparable to those of other apparatus, such as multipass cells or Cavity-Enhanced Absorption Spectroscopy techniques, but with a generally simpler set-up. Finally PA sensors present the advantages of a high dynamic range and the possibility to work at atmospheric pressure.

To improve the sensitivity of the system, resonant cell schemes can be used, exploiting most of the time radial, azimuthal or longitudinal resonance of acoustic waves. The cell that will be described in this paper is based on a differential Helmholtz resonance [4]. The modeled cell is presented in Figure 1.

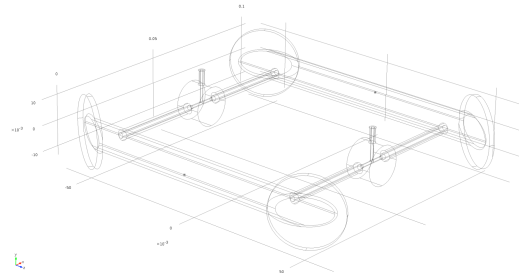


Figure 1. Schematics of the differential Helmholtz acoustic resonator modeled in this study

Two volumes (10 cm length, 1 cm diameter) linked by two capillaries (8 cm length, 0.2 cm diameter) form this PA cell. The gas in the capillaries moves like a piston, compressing gas in one volume whereas dilating it in the other. Consequently, acoustic waves are opposite in phase at resonance and by measuring it with two microphones (one in each volume), differential measurement is obtained: the difference of the two signals eliminates a great part of the acoustic noise and rises by a factor 2 the acoustic signal itself. The two capillaries enable to do flow measurements, as each of them is supplied with a valve, linked on one side to vacuum pumping system, on the other to atmosphere.

In photoacoustic spectroscopy, the light must be modulated at acoustic frequency to generate a signal in the cell. PA signal is linked to Beer-Lambert law [1]:

$$S_{PA} = \frac{RW}{L} (1 - \exp(-\alpha L)) \quad (1)$$

R is the total cell response, W the laser power, L the cell length and α the gas absorption. For low concentrations of absorbing molecules the PA signal is then equal to:

$$S_{PA} = RW\alpha \quad (2)$$

The gas absorption is linked with the concentration C of the molecules in air and to the absorption coefficient K_n :

$$\alpha(\lambda) = CK_n(\lambda) \quad (3)$$

The total response cell is given by:

$$R = \frac{(\gamma - 1)LQR_m}{\omega V_c} \quad (4)$$

γ is the heat capacity ratio, Q the quality factor of the resonant cell, R_m the microphone sensitivity, ω the angular frequency and V the cell volume.

Usually this total cell response is not calculated using this last equation but is obtained by using calibrated mixtures in the cell and measuring the obtained photoacoustic signal [5]. This paper will demonstrate the possibility to calculate complicated cell's response using the "Acoustics" module of Comsol Multiphysics®.

Moreover, in the framework of the ANR ECOTECH project "MIRIADE" the Helmholtz resonant photoacoustic cell presented here will be reduced to the millimeter range size. In order to predict the response of such a reduced cell we plan to use the "Thermoacoustics" module. A preliminary result using this module will be presented here.

2. Use of COMSOL Multiphysics

The theoretical description of sound generation in photoacoustic cells has been given in the 70s by several authors [6-7] and is summarized here. According to [8], the heat produced in a photoacoustic cell by light absorption represents the source for sound wave. Therefore a corresponding source term has to be added to the Helmholtz equation:

$$\nabla^2 p(\vec{r}, \omega) + k^2 p(\vec{r}, \omega) = i\omega \frac{\gamma - 1}{c^2} H(\vec{r}, \omega) \quad (5)$$

where p is the Fourier transform of the acoustic pressure, $k = \omega/c$ and c is the sound velocity. γ denotes the ratio of the specific heat at constant pressure C_p to specific heat at constant volume C_v . Assuming that the absorbing transition is not saturated, and that the modulation frequency is considerably smaller than the relaxation rate of the molecular transition, the relation $H(\vec{r}, \omega) = \alpha I(\vec{r}, \omega)$ applies where $I(\vec{r}, \omega)$ is the Fourier transformed intensity of the electromagnetic field. It is well known that the solution of the inhomogeneous wave equation

can be expressed as the superposition of the acoustic modes of the photoacoustic cell:

$$p(\vec{r}, \omega) = \sum_j A_j(\omega) p_j(\vec{r}) \quad (6)$$

The modes $p_j(\vec{r})$ and the corresponding eigenfrequencies $\omega_j = c k_j$ can be obtained by solving the homogeneous Helmholtz equation:

$$\nabla^2 p(\vec{r}) + k^2 p(\vec{r}) = 0 \quad (7)$$

It is assumed that the walls of the photoacoustic cell are sound hard, which leads to the boundary condition:

$$\frac{\partial p}{\partial n} = 0 \quad (8)$$

i.e., the normal derivative of the pressure is zero at the boundary. To use Eq 6, it is necessary to normalize the modes according to

$$\int_{V_c} p_i^* p_j dV = V_c \delta_{ij} \quad (9)$$

where V_c denotes the volume of the photoacoustic cell and p_i^* the complex conjugate of p_i .

When the acoustic modes p_j can be determined, the amplitude for each mode is expressed as

$$A_j(\omega) = i \frac{A_j \omega}{\omega^2 - \omega_j^2 + i\omega\omega_j/Q_j} \quad (10)$$

with

$$A_j = \frac{\alpha(\gamma - 1)}{V_c} \int_{V_c} p_j^* I dV \quad (11)$$

and

$$1/Q_j = 1/Q_j^v + 1/Q_j^{s_\kappa} + 1/Q_j^{s_\eta} \quad (12)$$

The inhomogeneous Helmholtz equation (Eq. 5) does not contain terms that account for loss. Loss effects are included via the introduction of quality factors Q_j in the amplitude formula (10). Several loss mechanisms occur in photoacoustic cells: volume loss, thermal and viscosity surface losses. Following [7], volume loss is simply due to energy transferred from the acoustic wave to thermal energy through heat conduction and through the viscosity:

$$1/Q_j^v = \frac{\omega_j}{c} [l_\eta + (\gamma - 1)l_\kappa] \quad (13)$$

where l_η and l_κ are characteristic lengths respectively defined by:

$$l_\eta = \frac{4}{3} \frac{\eta}{\rho c} \quad (14)$$

$$l_\kappa = \frac{\kappa}{\rho C_p c} \quad (15)$$

with η being the viscosity and κ the thermal conductivity. ρ represents the gas density.

The surface loss occurs in a thin region near the walls that is composed of two layers of thicknesses d_η and d_κ given by:

$$d_\kappa = \sqrt{\frac{2\kappa}{C_p \rho \omega_j}} \quad (16)$$

$$d_\eta = \sqrt{\frac{2\eta}{\rho \omega_j}} \quad (17)$$

Near the wall, the expansion and contraction of the gas are isothermal due to the greater thermal conductivity of the wall, whereas they are adiabatic far from the walls. Acoustic losses from heat conduction occur in the layer of thickness d_κ where the gas behavior is partly adiabatic and partly isothermal.

$$1/Q_j^{s_\kappa} = \frac{1}{2} (\gamma - 1) \frac{d_\kappa}{V_c} \int_{S_c} |p_j|^2 dS \quad (18)$$

Similarly, at the wall surfaces, the tangential component of the acoustic velocity is zero because of the viscosity, while far from the wall it is proportional to the gradient of the acoustic pressure. Viscoelastic loss occurs in the region of thickness d_η :

$$1/Q_j^{s_\eta} = \frac{1}{2} \left(\frac{c}{\omega_j} \right)^2 \frac{d_\eta}{V_c} \int_{S_c} |\nabla_t p_j|^2 dS \quad (19)$$

According to this description, the first step for the determination of PA cell response is the obtention of the acoustic eigenmodes p_j which can be done analytically only in some specific cases. When the geometry of the cell is more complex, the analytical determination of the eigenmodes is not possible. An alternative description based on a circuit analogy to a

transmission line can be used. However this kind of simulation is limited since it usually requires some empirical adjustments.

The progresses in numerical methods and the availability of user-friendly software using FEM open the way to direct resolution of the Helmholtz equation and to the optimization of photoacoustic cell's response. We present here an example of resolution of this equation for a Differential Helmholtz Resonant (DHR) photoacoustic cell with a complex geometry and its analysis using numerical simulation.

3. Main results

The "Acoustics" module of Comsol Multiphysics has been used to determine resonant frequencies, eigenmodes and quality factors determination. Baumann et al perform [9] a careful comparison between analytical determination and FEM simulation using Comsol Multiphysics 3.5 software for a cylindrical cell and found a good agreement for the eigenfrequencies and for the Q factors. They also perform a comparison between FEM simulation and experiment for T-shaped resonators that shows also a good agreement for eigenfrequencies and Q factors.

In order to analyze our DHR cell, we built a model with Comsol 4.2 software to perform the eigenvalues determination, their normalization and the calculation of the amplitudes A_j and of the various losses. A typical mesh of the photoacoustic cell is presented on Fig. 2 and the acoustic pressure repartition that corresponds to the Helmholtz eigenmode is shown in Figure 3.

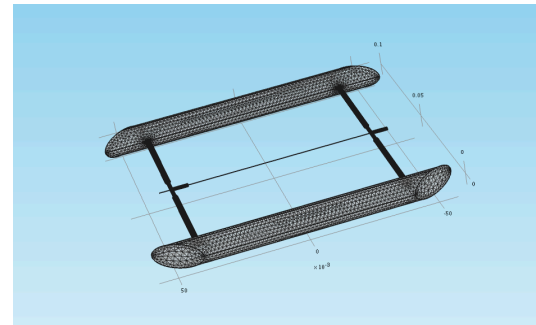


Figure 2. Typical mesh of the DHR cell

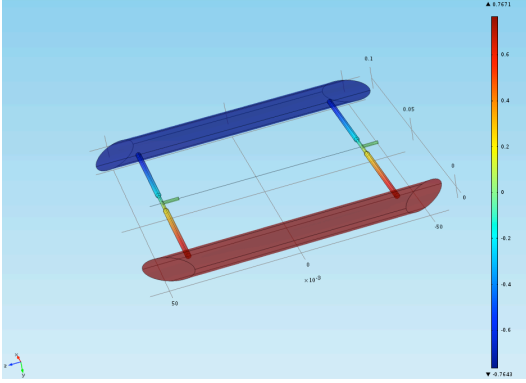


Figure 3. Acoustic pressure repartition for the Helmholtz eigenmode

The DHR is excited by a modulated laser beam propagating along one of the two cell volumes. The experimental Helmholtz resonance was found at 215 Hz whereas the eigenfrequency determined by the simulation is 215.35 Hz.

The model was used to obtain the pressure wave amplitude in both the excited and the non-excited volume of the cell. Calculations corresponding to Eq. (6) and (10) are performed using a Matlab® script. The comparison of simulation with measurements for the resonant geometry of Fig. 1 is plotted on Fig. 4. The model perfectly fits the experimental points.

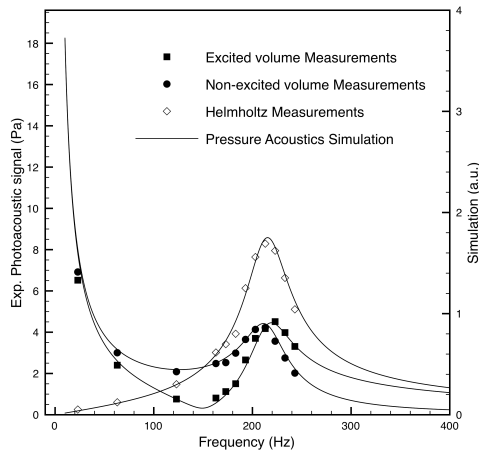


Figure 4. Comparison of experimental points with simulation using “Acoustics” module

Finally the same type of calculations was developed using the “Thermoacoustics” module. The objective is to demonstrate the correct description of this type of resonators previously to the reduction of the DHR to the millimeter range size in the framework of the ANR ECOTECH project “MIRIADE”. In the mm range case the geometric cell dimensions will become shorter than the wavelength and in the same order of magnitude than the viscous and thermal boundary layers. In such conditions the “Pressure Acoustics” equations do not apply. The interfaces under the Thermoacoustics module are used to accurately model acoustics in geometries with small dimensions. Near walls, viscosity, and thermal conduction become important, resulting in an acoustic boundary layer where losses are significant, making it necessary to include thermal conduction effects and viscous losses explicitly in the governing equations. Because detailed descriptions are needed to model thermoacoustics, all the interfaces simultaneously solve for the acoustic pressure p , the particle velocity vector \mathbf{u} , and the acoustic temperature variations T . Here is a summary of the main equations in this module:

$$\nabla \cdot \frac{1}{\rho_c} (\nabla p_t - \mathbf{q}) - \frac{k_{eq}^2 p_t}{\rho_c} = Q$$

$$i\omega \rho_0 \mathbf{u} = \nabla \cdot \left(-p_2 \mathbf{I} + \mu (\nabla \mathbf{u} + (\nabla \mathbf{u})^T) - \left(\frac{2}{3} \mu - \mu_B \right) (\nabla \cdot \mathbf{u}) \mathbf{I} \right)$$

$$i\omega \left(\frac{\partial \rho_0}{\partial p_2} p_2 + \frac{\partial \rho_0}{\partial T} T \right) + \rho_0 \nabla \cdot \mathbf{u} = 0$$

$$i\omega \rho_0 c_p T = -\nabla \cdot (-k \nabla T) - i\omega p_2 \frac{T_0 \partial \rho_0}{\rho_0 \partial T}$$

A preliminary result of simulation for the Fig. 1 Helmholtz resonant geometry is plotted on Fig. 5. One can remark the same type of obtained result than in Fig. 4. The Thermoacoustics interface is more dependent on the mesh quality. Thus the calculation time is typically 20 times greater than using the Pressure Acoustics interface. The use of the Thermoacoustics interface is not necessary to accurately model the macroscopic cell represented in Fig. 1 but will probably be mandatory for a miniaturized cell.

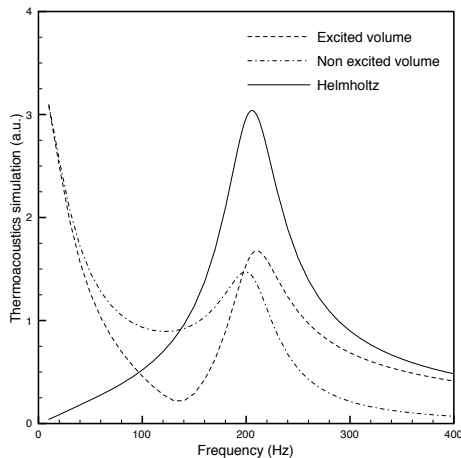


Figure 5. Preliminary result of Helmholtz resonator simulation using “Thermoacoustics” module

4. Conclusions

This paper has demonstrated the possibility to simulate a quite complicated Differential Helmholtz Resonator photoacoustic cell using Comsol Multiphysics® FEM software. After an introduction on photoacoustic principles, the major equations related to this phenomenon were presented. Resonant frequencies, eigenmodes and quality factors determination were determined using the “Acoustics” module of the Comsol Multiphysics 4.2. An excellent agreement was found with experimental points. In a second part a preliminary result obtained with the “Thermoacoustics” module was also presented. The same type of comportment than those obtained with “Acoustics” module is observed.

5. References

1. M.W. Sigrist, *Air Monitoring by Spectroscopic Techniques*, Wiley, New York (1994)
2. A. Grossel, V. Zeninari, B. Parvitte, L. Joly, G. Durry, D. Courtois, Photoacoustic detection of nitric oxide with a Helmholtz resonant quantum cascade laser sensor, *Infrared Physics and Technology*, **51**, 95-101 (2007)
3. A. Grossel, V. Zeninari, B. Parvitte, L. Joly, D. Courtois, Optimization of a compact photoacoustic quantum cascade laser

spectrometer for atmospheric flux measurements: Application to the detection of methane and nitrous oxide, *Applied Physics B: Lasers and Optics*, **88**, 483-492 (2007)

4. V. Zeninari, V.A. Kapitanov, D. Courtois, Y. N. Ponomarev, Design and characteristics of a differential Helmholtz resonant photoacoustic cell for infrared gas detection, *Infrared Physics and Technology*, **40**, 1-23 (1999)
5. V. Zeninari, B. Parvitte, D. Courtois, V.A. Kapitanov, Y.N. Ponomarev, Methane detection on the sub-ppm level with a near-infrared diode laser photoacoustic sensor, *Infrared Physics and Technology*, **44**, 253-261 (2003)
6. Y-H Pao, *Optoacoustic Spectroscopy and Detection*, Academic Press (1977)
7. A. Rosencwaig, *Photoacoustics and Photoacoustic Spectroscopy*, Wiley Interscience (1980)
8. P.M.Morse, K.U.Ingard, *Theoretical Acoustics*, Princeton University Press (1968)
9. B. Baumann, M. Wolff, B. Kost, H. Groninga, Finite element calculation of photoacoustic signals, *Applied Optics*, **46**, 1120-1125 (2007)

6. Acknowledgements

This work was funded by the ANR ECOTECH project #ANR-11-ECOT-004 called “MIRIADE” (2012-2014). Christophe Risser also acknowledges the Aerovia start-up (www.aerovia.fr) for his Ph.D funding by CIFRE contract.